Indian Journal of Radio & Space Physics
Vol 49, December 2020, pp. 162-170

Ionospheric responses to the consecutive earthquakes over Canadian sector

Emperumal Karthikeyan[a]*, Yasala Srinivas[a], Kaliappan Emperumal[b] & Sundararaman Sathishkumar[b]

[a]Centre for Geotechnology, Manonmaniam Sundaranar University, Abishekapatti, Tirunelveli, Tamil Nadu 627 012, India

[b]Equatorial Geophysical Research Laboratory, Indian Institute of Geomagnetism, Krishnapuram, Tirunelveli, Tamil Nadu 627 011, India

Received: 6 August 2020; Accepted: 15 October 2020

Recently, two successive earthquakes with the magnitude of 6.8 and 6.5 which have occurred at 200 km southwest of Port Hardy, Canada (49˚N, 129˚W) during October 2018 have been considered for our study. The TEC data has been acquired from nearby stations of these two events. It has been observed that an increase in TEC anomalies of about 0.1 TECU of moderate earthquake events occurred on the geo-magnetically quiet days. Besides, increases in the TEC anomalies have shown wave-like structures in the ionosphere and it may have associated with acoustic waves generated by earthquakes. The faulting mechanism of the earthquake and the propagation velocity of waves by TEC have confirmed the presence of acoustic wave activity.

Keywords: Total electron content (TEC), Co-Scismic Ionospheric disturbance (CID), Earthquake, Canada

1 Introduction

Earthquakes have occurred mainly along the plate boundaries, geologic fault zone, and shear zone areas with the release of energy that has induced the electronic charges to change and lead to the ionization of the lower atmosphere. More faults are active, associated with plate boundaries under the Eastern North Pacific Ocean West of British Columbia. Also, several earthquakes occur under the adjacent continental shelf, the Vancouver Island and the Strait of Georgia. The tectonic regime is controlled mainly by the motions of the Pacific, America, Juan de Fuca, and Explorer plates[1]. In the North of Vancouver Island, Queen Charlotte transform fault separates the Pacific and American plates. The Pacific plate has been separated by many ridges and faults from the Juan de Fuca plate and Explorer plate in the south. Regional tectonic activity has been dominated due to the convergence of plates between the Juan de Fuca plate and the North America plate. Baranova et al.[2] has stated that shallow earthquakes of depth below 30 km occur within the America plate whereas; the deeper earthquake event occurs within the sub-ducting the Juan de Fuca plate.

The faulting deformations mainly shear stress that has induced the wave as a source to perturb the ionosphere by propagating vertically upward. Gokhberg *et al.*[3] has reported that the ionosphere perturbations might be the propagation of internal gravity waves (IGWs) from the lower atmospheric processes such as seismic waves, atmosphere heating, and the injection of gases. Also, earthquakes have excited the atmospheric waves that propagated in the Earth's atmosphere[4-5]. Further, it may have perturbed the ionosphere layer which contains free electrons and positively charged ions and this manifestation can be identified by the total electron content (TEC). More evidence from past to the current times has suggested that the disturbances have occurred in the ionosphere (such as critical frequency, the peak electron density of F2 layer, and TEC) due to seismic signals and the disturbances have depended on the size of the earthquake[6-12]. A small displacement has been lead to vertical oscillations of several tens of meters at ionospheric height due to the surface Rayleigh wave. The continuity of vertical displacement and stress in the surface by acoustic and gravity waves has occurreddue to any earth events. The disturbances have occurred naturally in the ionosphere by different wavelengths as Ross by waves due to Coriolis Effect has a wavelength of 1000s of kilometres whereas; the acoustic gravity waves have travelled with the wavelength of 100 – 3000 km. The perturbation of ionosphere TEC has been one of the phenomena to couple the lithospheric events with the ionosphere and thereby the mechanism has been proposed in detail. Many researchers have noticed that the TEC gets

*Corresponding author (E-mail: ekarthikeyan2791@gmail.com)

amplified and has been used as a tool for precursory of the earthquakes and in our case also the disturbance has been observed after the event and has been named as co-seismic ionospheric perturbations. The amplitude has a variation of 0.2 – 0.4 TECU for the co-seismic perturbations to the shallow earthquakes of larger magnitudes. Different types of co-seismic perturbations in the ionosphere such as co-seismic crustal displacements by tsunami is and post-seismic have been caused by Rayleigh waves propagation[13-15]. The reason behind the mechanism of perturbation of the ionosphere has been discussed in detail in the results and discussion section and the TEC data has been processed and interpreted with detailed evidence.

2 Methodology

The strike-slip faulting occurs at shallow depths on the boundary of the explorer microplate and by fault, the plane identifies the strike, dip, and rake using the IRIS data[16]. The earthquake's impact on the ionosphere region and the variation is observed in the Total Electron Content (TEC) with the data obtained for the stations near to the epicenter from the International GNSS Service (IGS)[17]. Figure 1 indicates the epicenter of the earthquake (shown by a red star) and the IGS stations (shown by yellow triangle) nearer to the location of earthquake taken for the study. The surface Rayleigh wave leads to the displacement in the ionosphere region mainly to the

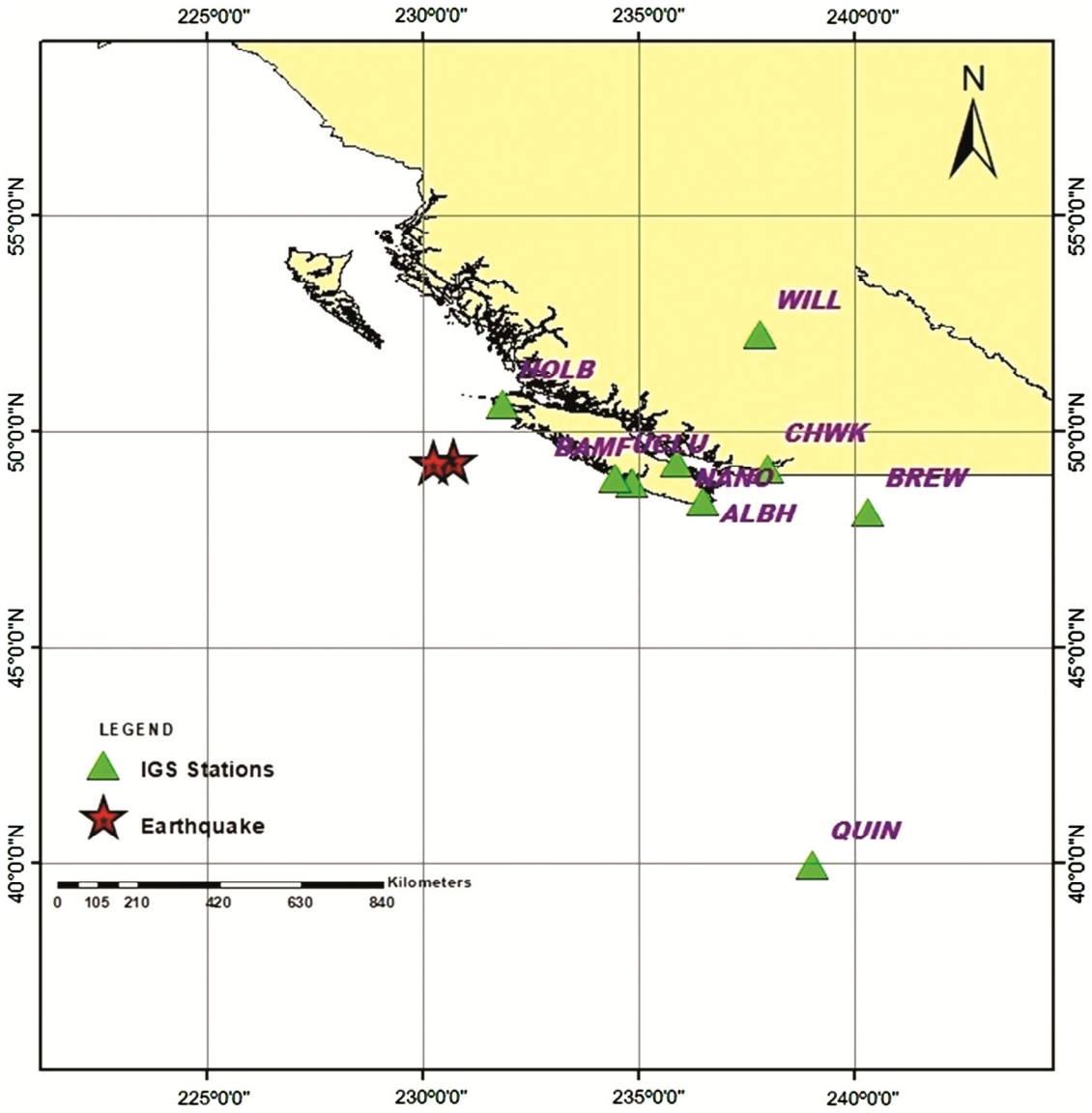

Fig. 1 — Distribution of GPS stations (green triangles) and epicenter of earthquakes (red star) of Magnitude 6.8 and 6.5 occurred on 22nd October 2018.

nearby stations concerning the size of the earthquake. Thereby the TEC in the ionosphere region can be considered for noticing the consistent changes in the ionosphere during, before and after earthquake occurrences. Rinex observation data have been used for the estimation of Slant Total Electron Content (STEC) for every 30 seconds of all nearby stations available; necessary corrections (viz. transmitter and receiver bias corrections) has been done for the accurate measurement of TEC associated with GPS observations. Figure 2 shows the satellite path with the time during the travel for the PRN 28 of every station taken for the study which passes near to the epicenter (indicated as the star) during the day of the earthquake. To confirm the geomagnetic quiet day, the DST index obtained from the World Data Centre (WDC)[18] and in support Solar Index (F10.7) data from the GSFC/SPDF OMNI Web interface[19] also utilized.

3 Results and Discussion

3.1 Description of earthquake and its mechanism

Pacific plate motion with respect to the North America plate towards the northwest motion at a velocity of 50 mm/year results in the active tectonic activities of the Pacific margin of North America

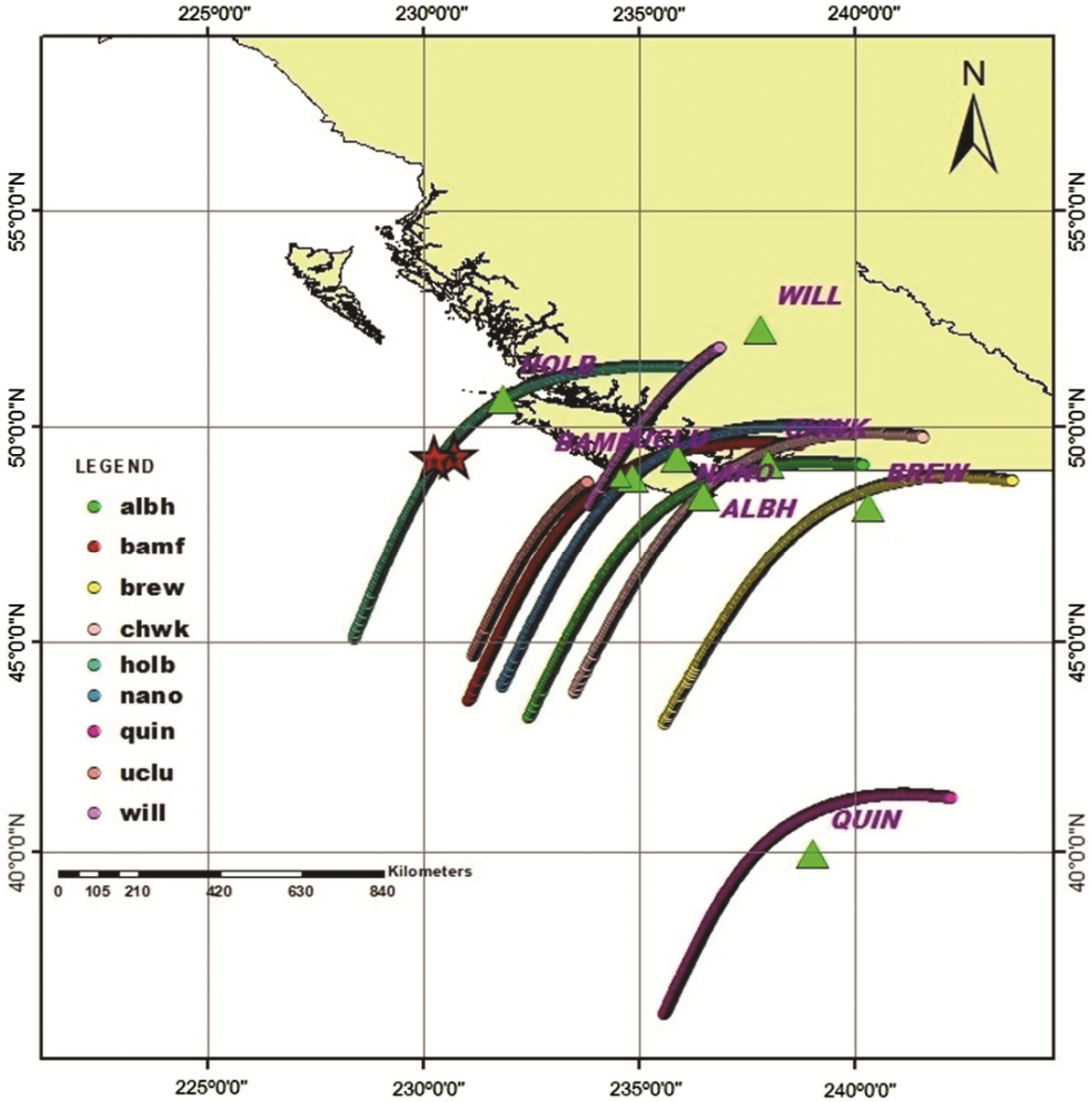

Fig. 2 — Trajectories of ionospheric pierce points for certain satellites of PRN 28 for all stations and other things indicated in Fig. 1.

between Vancouver Island and South – Central Alaska. The convergence of plates between the Juan de Fuca plate and the North America plate dominates the regional tectonic activity. Due to this tectonic activity, a moderate earthquake occurs frequently in this region because of the internal dextral faulting deformation and recorded a maximum of 6.8 Mw earthquakes since 1980. The consecutive earthquakes of 6.8 and 6.5 Mw were recorded within minutes and fall under the moderate earthquake zone[20]. The earthquake of magnitude 6.8 seems to strike-slip faulting with the strike and dip angle of 309º & 80º for nodal plane 1 and 218º & 84º for nodal plane 2 respectively. The focal mechanism indicates the vertical northwest-southeast striking fault and indicates the direction of rupture that occurred.

3.2 Geomagnetic conditions

The ionosphere variation is due to different parameters like sunspot number, DST index, ap index, F10.7, and so on. The above said parameters have been observed to confirm the geomagnetic quiet conditions with the results which are shown in Fig. 3. The black vertical line indicates the day of the earthquake event occurred. Firstly, (Fig. 3(a) indicates the DST index and observed the range falls within the limit of ±20 nT by giving the way to confirm the quiet geomagnetic condition. Also, (Fig. 3(b) indicates the ap index confirms the quiet to slight moderate condition and falls in the range of 0 to 5 nT. This geomagnetic quiet condition gives the enhanced results and the quiet condition helps to study the earthquake effects in the ionosphere and hence the results are fashioned in a better way.

3.3 Behaviour of TEC

The Total electron content (TEC) presents in the ionosphere region resulted in variations during external (solar flare, geo-magnetically disturbed day) and internal (earthquake, volcanic eruptions, and cyclone) conditions. The TEC indicated the primary changes in the ionosphere and the study dealt with the observation during the time of the earthquake. Here, the earthquake was considered to be the source of ionosphere variation and the stations shown in Fig. 1 were considered which is nearer to the epicenter and taken for observation of TEC. The disturbance in the ionosphere was detected using Total Electron Content (TEC) where the periodic oscillations have been seen after the earthquake (Example: 2009 observed for the Sumatra earthquake[21,22], 2011 for Tohoku Earthquake[12,23], 2016 for New Zealand earthquake[24] and many more). Likewise, the observation of TEC seems to be varied for all nearby stations in the vicinity of the epicenter.

The disrupture in the rocks and the plate boundaries during earthquake released the energy wave which travel to the atmosphere through different mechanisms. Generally, the greater earthquakes result in exciting more waves to the atmosphere and travel to a longer distance while in our case the two moderate earthquakes are considered. So, the energy released during the earthquake gave rise to some extent for vertical propagation with respect to the distance. In

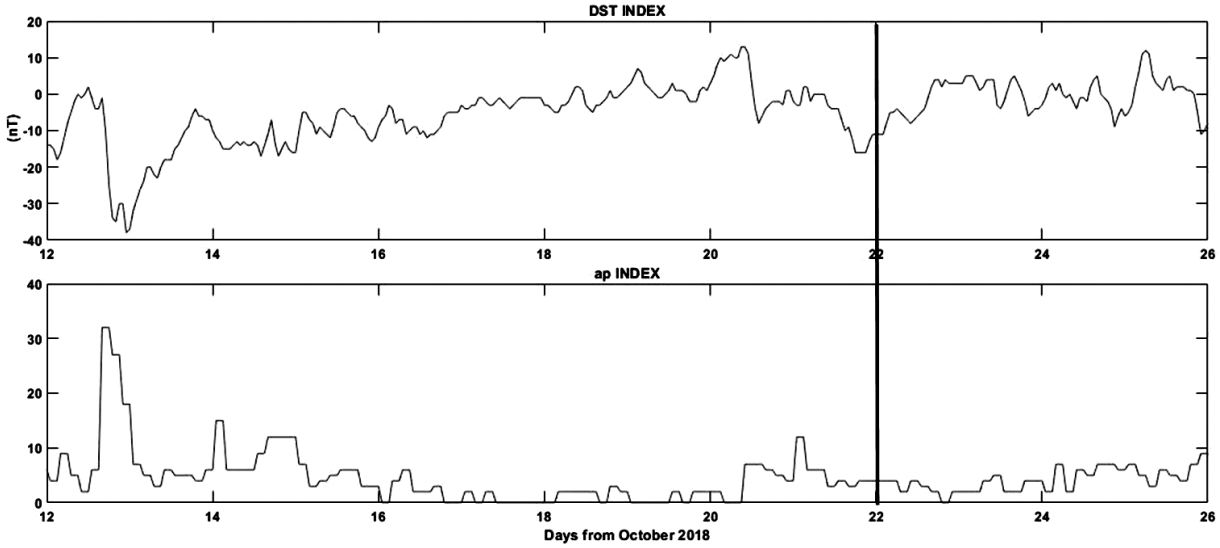

Fig. 3 — a) DST index and b) ap index for the period of 12th October to 25th October 2018 and the black vertical line indicates the day earthquake occurred.

the present case, we have considered the distance of 1000 kilometres of radius from the epicentre for the selection of stations to observe the TEC variations. The TEC data was taken every 30 seconds for better results and seen the variations particularly on earthquake day (i.e. 22nd October 2018). The irregular variation of TEC observed for different stations and various satellites are identified using the Pseudo Random Number (PRN) Sunil *et al.*[25] adopted the same way as Bagiya *et al.*[8] for the perturbations caused by the acoustic signal. Here, the different PRN's of satellite is considered and the notable changes in TEC seen for the PRN 28 (Fig. 2 indicates the travel path of satellites) while others are not considered because of distance from epicenter (far away data points are not considered as the event falls under moderate magnitude earthquake). To see the earthquake effect on ionosphere the previous and post-seismic days (i.e. quiet day) are considered and the dramatic changes are seen only during the earthquake day and not on other days. As seen in Fig. 4, the variations observed for all stations near the epicenter seem to have oscillations with the variation of ± 0.5 TECU during the earthquake.

The Co-seismic Ionospheric Disturbances (CID) was seen for all stations and significant changes were observed in PRN 28. We observed the different TEC variations with respect to the time of earthquake and by applying the low pass filter during the period of 6 UT to 7 UT for earthquake day and control day as shown in Fig. 4. The station HOLB, UCLU and WILL were observed to be very close to the epicentre and observed the variations of 0.1 TECU only on event day (i.e. 22nd October 2018). As the consecutive moderate earthquakes of nearly the same magnitude over the nearby region occurred within the minutes leads to the overlap of wave signatures. This wave signatures amplitude depends on the magnitude of earthquake and distance from the epicenter resulted in the variation of TEC for a period of 10 minutes in our study. The station BREW was observed to be 650 kilometres away from the epicenter noticed the N-type pattern of oscillations for the period of 7 minutes.

The TEC based studies[14] reported that the depletion of TEC followed by sudden enhancement lasts for the period of 10 minutes noticed on three large marine earthquakes. The station HOLB near the epicentre noticed only the small variations. The wave which propagates vertically not only above the epicenter and but also it depends on the fracture and while other lineaments in the rock also play a role. The oscillations were due to the acoustic waves which was vertically propagated from the lithosphere to the

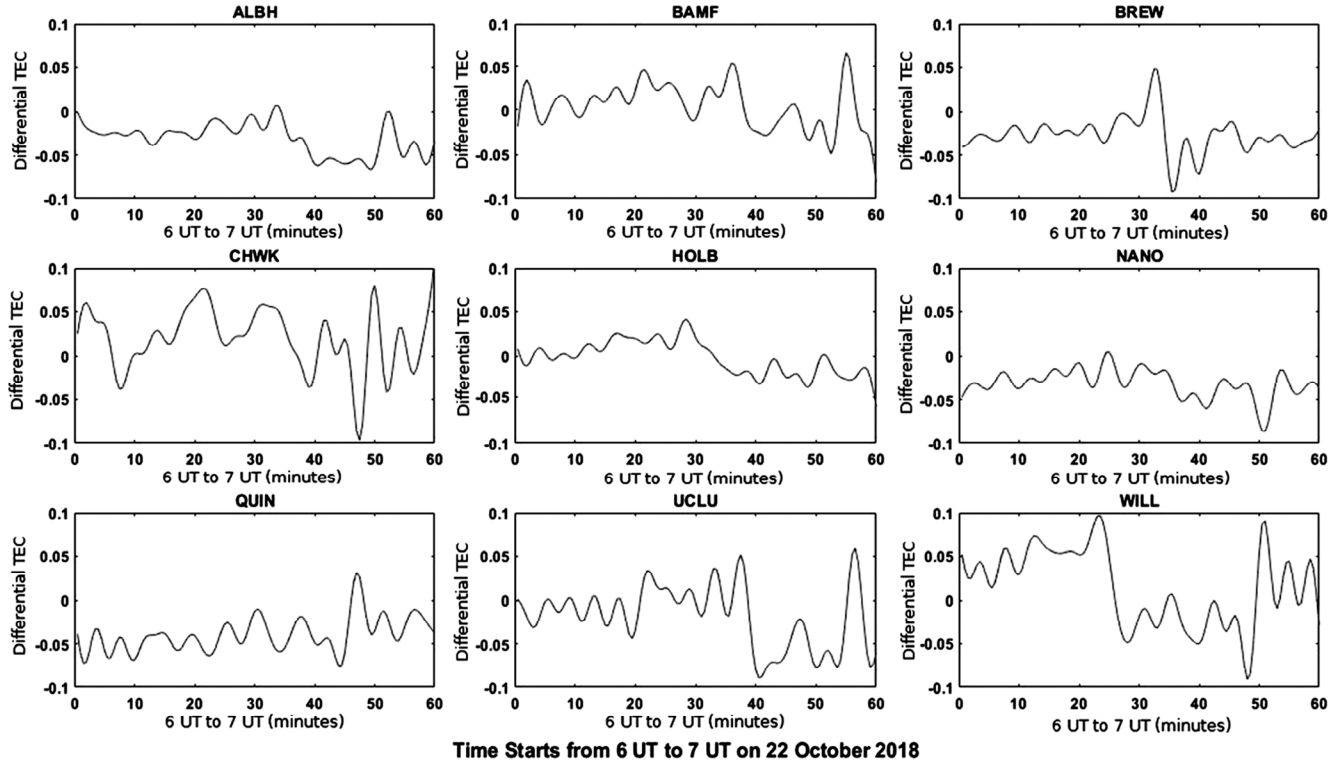

Fig. 4 — Differential TEC variations for all stations shown in Fig. 1 for the time period of 06 UT to 7 UT.

lower atmosphere by redistributing the plasma gives rise to the ionospheric perturbations[22,26]. In general, for strong earthquakes, the acoustic wave caused the disturbances with the duration of about 100seconds at altitudes with notable intensity even at a long distance from the epicenter[27]. While the other station also seemed to have slight variations and due to the distance amplitude of propagating waves gets decreased.

As the stations HOLB, UCLU and WILL were nearer to the epicenter, these stations observed the variations for TEC anomaly from the time of 06.30 UT onwards and continued for the period of 5 to 10 minutes with the overlapping of N-type oscillations and resulted in a different pattern. But some of the stations were farther apart from the epicenter and observed only the single peak of N-type pattern as like the large earthquake events due to the dissipation of weaker seismic signals. Param K. Gautam *et al.*[15] reported that as the distance increases the energy of acoustic waves generated dissipated in the lower atmosphere itself and hence less effect were taken place in the electron redistribution which could not be seen much change for smaller magnitude and high focal depth earthquakes and also PRN of any station having distance more than 1000 km.

The variation seemed to be -0.1 TECU to +0.1 TECU significantly for the nearby stations while the farther observed -0.5 TECU to +0.5 TECU. At the same time, the propagation speed and direction of the wave also played a role in TEC variation and the same observed for the station HOLB. The TEC variations with maximum amplitude were observed for the stations at the southern side of the epicenter with the wave propagation velocity of 0.6 km/s whereas; the dissipation on the other side is noticed. The reason for small perturbation in the ionosphere for the nearby station was caused by geomagnetic field as the directivity effect prohibits the propagation of Northward propagation in Northern Hemisphere Heki and Ping[28]. As the perturbations were noticed due to the wave-like signature and also studied in detail about the direction of propagation. In all stations, the co-seismic ionospheric perturbations obtained as N-type wave pattern was consist of high compression and rarefaction. The wave propagated upward through the inhomogeneous atmosphere (the atmosphere is a viscous medium with decreasing density) transforms into a shock-acoustic wave where the wave amplitude increased due to non-linear effects[29]. The directivity effect complicated the interpretation of signals observed over northward from epicenter because the acoustic wave propagated on both northwards and southwards with respect to epicenter moves the plasma upward and downward in different ways. Heki and Ping[28], Gokhberg *et al.*[30] stated that in some cases, the northwards of epicenter can be noticed negative phase of the N-type wave propagated with the acoustic speed in the upper ionosphere and the same was resulted in our study.

3.4 Acoustic wave propagation and disturbances in ionosphere

The wave propagation and the influence of ionospheric TEC variation with respect to the distance were visualized using 3D for better understanding and shown in Fig. 5. The red star indicates the epicenter of earthquake whereas, the 3D contour was observed to be the variation of TEC anomaly after the earthquake along the direction of latitude and longitude. To understand the strong seismic signal this gave rise to acoustic wave propagation in the vertically upward direction from different stations during the time of 6.20 UT to 6.40 UT with a distance of 400 km from epicenter. The propagation of waves significantly increased the TEC variation towards the longitudinal direction to the vicinity of a 1000 km radius. The wave propagation from the epicenter to certain heights of the atmosphere was depended on the amplitude of the acoustic wave and direction of wind during the wave propagation. Bagiya *et. al*.[8] stated that the propagation of acoustic wave distance released from the epicenter was derived by the ray-tracing method and the distance was around 300 km. The change in TEC anomalies was noticed for certain magnitudes with the help of GPS station selection to estimate the extent of disturbances in the ionosphere with relation to the earthquake. The magnitude 6.2 of the Tajikistan earthquake resulted in a major effect upto the distance of 500 to 600 km from the epicenter and gets minimal beyond 600 km from epicenter[31]. Here we noticed the same result that the effect of TEC disturbances was seen for the distance of 600 km and beyond that distance the dissipation lead to the minimal effect of TEC anomalies.

The TEC anomaly with respect to time and epicentral distance is given in Fig. 6 for clear understanding. The variation seen after the time of

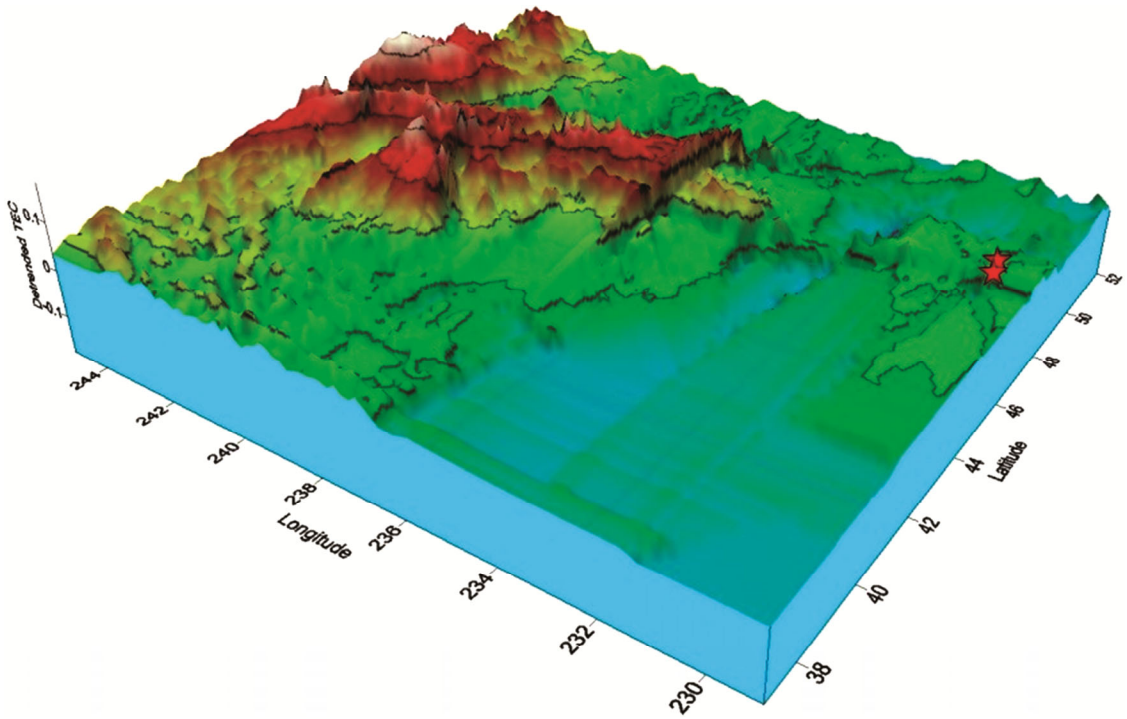

Fig. 5 — Longitude and Latitude variation of TEC in 3 dimension and red star indicates the epicenter of earthquake.

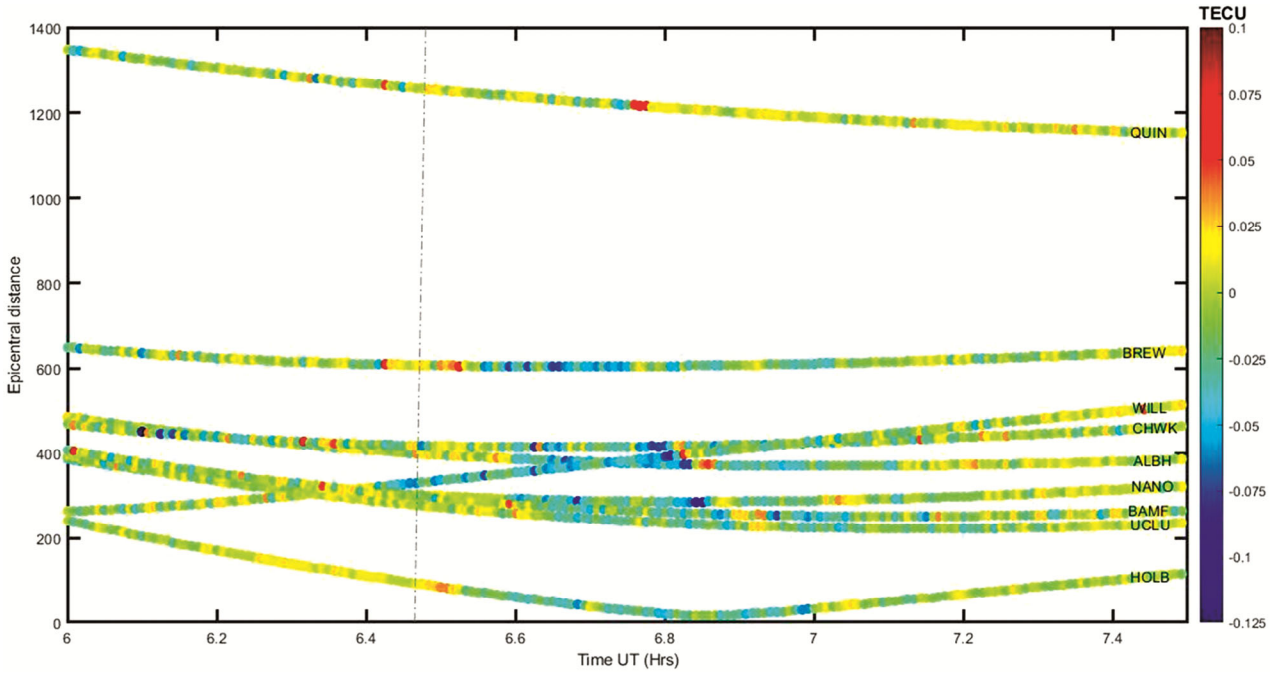

Fig. 6 — TEC anomaly with respect to the epicentral distance and time.

earthquake occurrence and the propagation of acoustic wave velocity can be roughly determined as 0.6 km/s with the model. The fluctuations of 0.1 TECU were observed for this moderate earthquake and the intensity of anomaly increased with the magnitude and decreased with the increase in focal depth. Mutschlecner and Whitakesdr[32] observed that infrasonic and acoustic gravity waves were excited during shallow earthquakes which could propagate to the atmospheric layer. These acoustic gravity waves

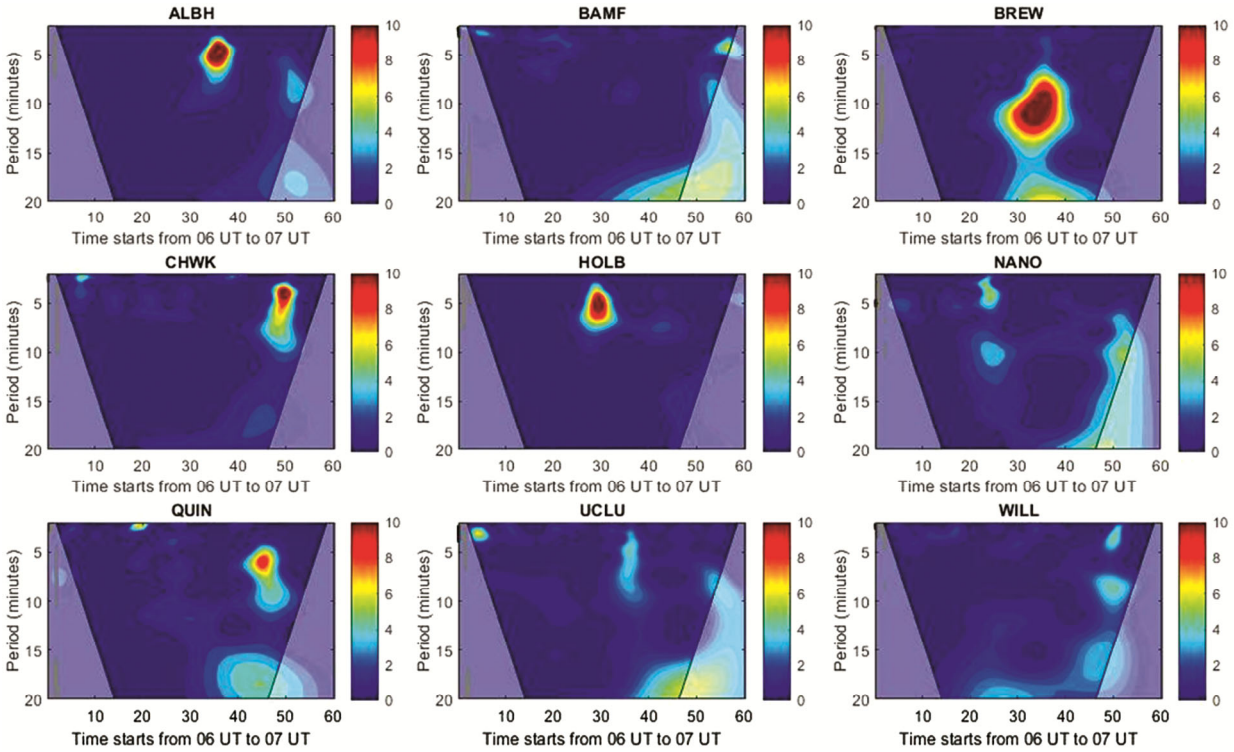

Fig. 7 — Morlet Wavelet analysis for the stations to derive the gravity waves on 22nd October 2018.

propagated to the ionospheric altitudes and collapsed the electron density[33]. The generated atmospheric gravity waves travelled great distances by propagating upward direction and the neutral particles induced fluctuations of ionospheric electron density. These seismically induced fluctuations were observed for the ionospheric parameter of TEC and caused the reduction due to the outflow of electrons and ions on earthquake time[11]. For the evidence of gravity waves propagation, we utilized the morlet wavelet analysis technique and were shown in Fig.7. Chimonas and Hines[34] stated that the vertical propagation of gravity waves was observed when the vertical wave number was real and the magnitude of intrinsic frequency was less than the Brunt-Vaisala frequency and calculated using the equations presented by Jones[35]. We observed the frequency of ~ 3 MHz which showed the prominent signature during 6:30 to 6:45 UT over BREW at the time of the earthquake's occurrence. An interesting feature was observed that the detrended TEC approached the quiet hour values both before and after earthquakes. As the waves were noticed in all the stations during the time of 06.30 UT for the nearby stations while far away stations observed on 06.45 UT approximately with the frequency range ~ 2 to 3 MHz which was probably associated with acoustic gravity waves. The station BREW observed the strong wave activity and in the same manner, the stations ALBH, CHWK and HOLB also seen strong variations.

4 Conclusions

In the present study, we have examined the ionospheric responses to the moderate earthquake event over the Canadian sector. It has been observed that TEC has shown an increase of about 0.1 TECU associated with moderate earthquake activity. However, the TEC has varied during the earthquake time for the time period of 10 minutes with the frequency range of 3 MHz when the seismic activity has triggered in the Canadian region. In this case, the parallel forces that have been applied to the fault (i.e. strike-slip) surface have resulted in the emission of an electron and the rate of emission has depended on the magnitude of the earthquake and the pressure applied on the fault surface. This has resulted in the ionospheric changes by different types of seismic waves such as infrasonic waves and acoustic gravity waves which have been stimulated by vertical movement of the earth's surface Rayleigh wave. The generated acoustic gravity waves have been slightly tilted upwards from the focal area and have causeda

change in the direction of propagation[36-37]. The wave activity has been observed to be dominant within the minutes of the earthquake's occurrence and it has also depended on the distance of a station from the epicenter. The average velocity of acoustic wave propagation has based on the occurrence and direction of CID from the epicenter to the ionosphere. The co-seismic ionospheric disturbances have depended mainly on the dense GPS network. Since, the earthquake has occurred in the sea, it has been a hindrance in locating the exact source of perturbation. The presence of acoustic frequency waves has confirmed the result of the ionospheric TEC disturbances. Also, the mechanism that have involved in coupling to study different height from lithosphere to ionosphere has been required to utilize the ground and satellite based instruments.

Acknowledgement

E Karthikeyan is very much grateful to the Director, Indian Institute of Geomagnetism (IIG), Mumbai for the grants under Dr. A. P. J. Abdul Kalam Fellowship. GPS TEC analysis software is obtained from Dr. Gopi K. Seemala, (IIG) is gratefully acknowledged.

References

1 Adams J & Clague J J, *Progress in Physical Geography*, 17(2) (1993) 248.
2 Baranova V, Mustaqeem A and Bell S, *Can J Earth Sci,* 36 (1999) 47.
3 Gokhberg M B, Nekrasov A K & Shalimov S L, *Physics of the Earth*, 8 (1996) 52.
4 Artru J, Farges T & Lognonné P, *Geophysical Journal International*, 158 (3) (2004) 1067.
5 Blanc E, *Ann Geophys*, 3 (1985) 673.
6 Afraimovich E L, Perevalova N P, Plotnikov A V & Uralov A M, *Ann Geophys*, 19 (2001) 395.
7 Afraimovich E L, Kirushkin V V & Perevalova N P, *J Commun Technol Electron*, 47 (2002) 739.
8 Bagiya M S, Sunil A S, Sunil P S, Sreejith K M, Rolland L & Ramesh D S, *J Geophys Res Space Physics*, 122 (2017) 6849.
9 Bolt B A, *Nature*, 202 (1964) 1094.
10 Calais E & Minster J B, *Geophys Res Lett,* 22 (1995) 1045.
11 Liu J Y, Chen Y I, Chen C H, Liu C Y, Chen C Y, Nishihashi M, Li J Z, Xia Y Q, Oyama K I, Hattori K & Lin C H, *J Geophys Res Space Physics,* 114 (4) (2009) A04320.
12 Saito A, Tsugawa T, Otsuka Y, Nishioka M, Iyemori T, Matsumura M, Saito S, Chen CH, Goi1 Y & Choosakul N, *Earth Planets and Space,* 63 (2011) 863.
13 Astafyeva E, Lognonné P & Rolland L, *Geophys Res Lett*, 38 (2011) L22104.
14 Kakinami Y, Kamogawa M, Tanioka Y, Watanabe S, Gusman A R, Liu J Y, Watanabe Y & Mogi T, *Geophys Res Lett*, 39 (2012) L00G27.
15 Gautam P K, Chauhan V, Sathyaseelan R, Kumar N & Pappachen J P, *NRIAG Journal of Astronomy and Geophysics*, 7 (2) (2018) 237.
16 (http://ds.iris.edu/wilber3/).
17 (http://garner.ucsd.edu/pub/rinex/2018/).
18 (http://wdc.kugi.kyoto-u.ac.jp).
19 (https://omniweb.gsfc.nasa.gov/ form/dx1.html).
20 (https://earthquake.usgs.gov/).
21 Choosakul N, Saito A, Iyemori T & Hashizume M, *J Geophys Res*, 114 (2009) A10313.
22 Shinagawa H, Iyemori T, Saito S & Maruyama T, *Earth, Planets and Space*, 59 (2007) 1015.
23 Heki K, *Geophys Res Lett*, 38 (2011) 1585.
24 Bagiya M S, Sunil P S, Sunil A S & Ramesh D S, *Journal of Geophysical Research: Space Physics*, 123 (2018) 1477.
25 Sunil A S, Bagiya M S, Reddy C D, Kumar M & Ramesh D S, *Earth, Planets and Space*, 67 (37) (2015).
26 Sunil A S, Bagiya M S, Catherine J, Rolland L, Sharma N, Sunil P S & Ramesh D S, *Advances in Space Journal,* 59 (5) (2017) 1200.
27 Orlov V V & Uralov A M, *Nauka,* 78 (1987) 28.
28 Heki K & Ping J, *Earth and Planetary Science Letters*, 236 (2005) 845.
29 Zel'dovich Ya B & Raizer Yu P, *Journal of Fluid Mechanics,* 31(4) (1968) 826.
30 Gokhberg M B, Lapshin V M, Steblov G M & Shalimov S L, *Atmospheric and Oceanic Physics*, 47(9) (2011) 1019.
31 Sharma G & Raju P, *Coordinates,* 15(7) (2019) 14.
32 Mutschlecner J P & Whitaker R W, *J Geophys Res,* 110 (1) (2005) 1.
33 Calais E & Minster JB, *Physics of the Earth and Planetary Interiors*, 105 (1998) 167.
34 Chimonas G H & Hines C O, *J Geophys Res*, 91 (1986) 1219.
35 Jones R M, *J Geophys Res*, 111 (D6) (2006) D06109.
36 Astafyeva E, Heki K, Kiryushkin V, Afraimovich E & Shalimov S, *J Geophy. Res,* 114 (2009) A10307.
37 Hickey M P, Schubert G & Walterscheid R L, *J Geophys Res,* 114 (2009) A08304.